

Functional characterization of the Ca²⁺-ATPase SMA1 from *Schistosoma mansoni*

Xavier Maréchal^{1,2,3}, Ricardo De Mendonça⁴, Roger Miras^{1,2,3}, Jean Revilloud⁵, Patrice Catty^{1,2,3*}

¹Université Grenoble Alpes, F-38054 Grenoble, France.

²CNRS, Laboratoire de Chimie et Biologie des Métaux, UMR 5249, 17 rue des Martyrs, F-38054 Grenoble, France.

³CEA, DRF, BIG, F-38054 Grenoble, France.

⁴Hôpital ERASME, Cliniques Universitaires de Bruxelles, ULB, Route de Lennik 808, B-1070 Bruxelles

⁵Institut de Biologie Structurale, 71 avenue des Martyrs, CS 10090, 38044 Grenoble Cedex 9

* Corresponding author: E-mail: patrice.catty@cea.fr

Short title: Functional characterization of SMA1

Key words: P-type ATPase, calcium, *Schistosoma mansoni*, thapsigargin, acid cyclopiazonic

Abbreviations: TG: thapsigargin; CPA: acid cyclopiazonic; SR: sarcoplasmic reticulum; PLN: phospholamban; E-strain: strain expressing *SMA1*; NE-strain: non-expressing strain; Tm: transmembrane helix

ABSTRACT

Schistosoma mansoni is a parasite that causes bilharzia, a neglected tropical disease affecting hundreds of millions of people each year worldwide. In 2012, *S. mansoni* had been identified as the only invertebrate possessing two SERCA-type Ca²⁺-ATPases, SMA1 and SMA2. However, our analysis of recent genomic data shows that the presence of two SERCA pumps is rather frequent in parasitic flatworms. To understand the reasons of this redundancy in *S. mansoni*, we compared SMA1 and SMA2 at different levels. In terms of sequence and organization, the genes *SMA1* and *SMA2* are similar, suggesting that they might be the result of a duplication event. At the protein level, SMA1 and SMA2 only slightly differ in length and in the sequence of the nucleotide binding domain. To get functional information on SMA1, we produced it in an active form in *S. cerevisiae*, as previously done for SMA2. Using phosphorylation assays from ATP, we demonstrated that like SMA2, SMA1 bound calcium in a cooperative mode with an apparent affinity in the micromolar range. We also showed that SMA1 and SMA2 had close sensitivities to cyclopiazonic acid but different sensitivities to thapsigargin, two specific inhibitors of SERCA pumps. On the basis of transcriptomic data available in GeneDB, we hypothesize that SMA1 is a housekeeping Ca²⁺-ATPase whereas SMA2 might be required in particular striated-like muscles like those present the tail of the cercariae, the infecting form of the parasite.

INTRODUCTION

P-type ATPases are primary active transporters providing by ATP hydrolysis, the energy required for the predominantly metal transport process, otherwise thermodynamically unfavorable. ATP hydrolysis proceeds by several steps (E1-E2 cycle), among them the transient phosphorylation of the transporter by transfer of the γ -phosphate of ATP to an aspartate residue in the highly conserved DKTGT sequence[1]. As particularly well illustrated by many X-ray structures of the Ca²⁺-ATPase SERCA1a, P-type ATPases undergo important conformational changes during their catalytic cycle [2]. These changes which reflect a “crosstalk” between the catalytic and the transport parts of the protein allow ion or lipid motions from one side to the other side of the membrane.

Through their role in cell transportomes, P-type ATPases are probably essential in parasite development; as a corollary, these proteins might also constitute interesting therapeutic targets.

However, little has been published about parasite P-type ATPases. The few examples concern P-type ATPases from Plasmodium [3-5], Leishmania [6,7], Entamoeba [8] and Trypanosoma [9].

The present work focuses on the Ca^{2+} -ATPases of the parasite *Schistosoma mansoni*, the most widespread of the human-infecting schistosomes; human schistosomiasis or bilharzia is a neglected tropical disease that affects hundreds of millions of people each year worldwide [10]. Like many parasites, *S. mansoni* has a complex life cycle, involving three types of environments. In freshwater, worm eggs hatching liberates miracidia that later colonize snails. In the mollusk, miracidiae transform into sporocysts that multiply asexually and produce many swimming cercariae, the infecting forms of the parasite. Cercariae penetrate human skin and during this process, their heads transform into endoparasitic larvae called schistosomules. After few days in the skin, schistosomules enter bloodstream and then transform in several weeks into adult male and female worms that reproduce sexually and give a large number of eggs released in water by feces.

The first study of a P-type ATPase from *S. mansoni* dates back to 1986 with the first detection of a Na^+/K^+ -ATPase activity in a preparation from adult parasite tegument [11]. The localization of the Na^+/K^+ -ATPase was later confirmed by a proteomic approach [12] and the genes coding for the α subunit (SNaK1 α) and the β subunit (SNaK1 β) were cloned in 2001 and 2013 from an adult parasite cDNA library [13,14]. Ca^{2+} -stimulated, Mg^{2+} -dependent ATPase activities were measured for the first time in 1988 in different subcellular fractions of an adult parasite. In the microsomal fraction, this activity was characterized by an apparent $K_{1/2}$ for calcium comprised between 0.2 and 0.5 μM [15], a value later confirmed by $^{45}\text{Ca}^{2+}$ -uptake assays [16]. Vanadate, a broad spectrum inhibitor of P-type ATPases, but also thapsigargin (TG) and cyclopiazonic acid (CPA), specific of SERCA-type Ca^{2+} -ATPases (Sarco-Endoplasmic Reticulum Ca^{2+} -ATPases), were shown to fully inhibit the Ca^{2+} -ATPase activity in the microsomal fraction with half maximum effect at 2.5 μM , 250 nM and 0.8 μM , respectively [16,17]. In 1995, De Mendonça and collaborators, PCR-amplified four *S. mansoni* cDNA fragments (SmI to SmIV) using degenerated primers designed from conserved P-type ATPases motifs. *In silico* analyses revealed that SmI and SmII encodes parts of SERCA-type Ca^{2+} -ATPases, SmIII encodes a part of a SPCA-type Ca^{2+} -ATPase (Secretory Pathway Ca^{2+} -ATPases) and SmIV encodes a part of a Na^+/K^+ -ATPase [18]. In the genome of *S. mansoni* [19,20], *SMA1*, the full-length gene corresponding to SmI, is located on chromosome 1 (Chr1), at the Smp_007260.1 locus (GeneDB). *SMA2* is located on Chr3 at the Smp_136710 locus; *SMA2* is so far, the only biochemically characterized *S. mansoni* P-type ATPase [21]. *SMA3* is located on ChrZW at the Smp_126300 locus but encodes an amino acid sequence which differs from the published one [22] by the absence of 10 amino acids upstream the DKTGT motif and 38 residues in the P-domain (personal observation). *SMA3* was proposed to localize at the tegument of the adult worm [22]. Finally, SmIV would correspond to one of the two Na^+/K^+ -ATPase of *S. mansoni*, encoded by Smp_015020 on chr3 (personal observation).

It was noticed few years ago that *S. mansoni* was the only invertebrate with two SERCA-type Ca^{2+} -ATPases, *SMA1* and *SMA2* [23]. However, our analysis of recent genomic data shows that it would be also the case in many parasitic flatworms. In the present work, we addressed the question of this redundancy by comparing these two pumps at the genomic, transcriptomic and protein levels. We also determined some enzymatic properties of *SMA1* after its production *S. cerevisiae* and compared them to those of *SMA2* previously measured in similar conditions, using the Ca^{2+} -ATPase SERCA1a from the rabbit sarcoplasmic reticulum, as reference.

EXPERIMENTAL PROCEDURES

Chemicals and enzymes – TG, CPA and Na_2ATP were purchased from Sigma. All other compounds were of analytical grade. Restriction enzymes were obtained from New England Biolabs Inc.

Strains and media - *Saccharomyces cerevisiae* YPH 500 (Mat α , ura 3-52, lys 2-801 amber, ade 2-101 ochre, trp 1- Δ 63, his 3- Δ 200, leu 2- Δ 1, [24] was used as host for *SMA1* expression. Cultures were carried out at 30°C, either in rich medium containing 1% yeast extract (KAT, Ohly, Hamburg, Germany) and 2% glucose or in selective minimum dropout medium containing 2% glucose, 0.7%

yeast nitrogen base without amino acids and 0.13% dropout powder minus uracil (MP BioMedicals). The method of Kuo et al. [25] was used for yeast transformation.

Assembling of SMA1 cDNA and construction of the YEp195SMA1 vector – The SMA1 gene was obtained from a cDNA (λ gt10) and a genomic (EMBL3 vector) library as described in [18]. It was expressed in *S. cerevisiae* from the multicopy YEplac195 vector [26], under the control of the strong constitutive PMA1 promoter. To improve the expression level of SMA1, a specific linker was designed to recreate immediately upstream the ATG codon, an initiation region (Kozak sequence) identical to that of the strongly expressed yeast PMA1 gene. The construction of the vector YEp195PSA, used for the production of SERCA1a in yeast, is described in [27].

The phosphorylation site mutant – The D354A mutant, in which the aspartate residue phosphorylated during the catalytic cycle of the ATPase has been replaced by an alanine was made using the QuickChange Lightning site-directed mutagenesis kit (Agilent) and the following primers: Forward : TTTGTTCTGCAAAAACCGGTACCCT; Reverse : CCGGTTTTTGCAGAACAAATCACTG. In the yeast expression vector, the mutated SMA1 gene as well as the junctions with the PMA1 promoter and the ADH1 terminator were entirely sequenced (GeneWiz) using the following primers: CCCAGCTAGTTAAAGAAAATCATTG, CGGAACAAGATAAGACTCCTCTCGGGC, CCCTCAAAGTCAAATTTCCGGCTC and GACTGCTGCTCTCGGTATGCCTGAGG.

Northern analysis - Total RNA extraction from yeast strains containing YEp195PA or YEp195SMA1 was performed as described in [28]. Northern blotting was carried out with Hybond-N⁺ nylon membrane (Amersham). The hybridization was performed overnight at 42°C in the presence of 5x SSPE (5 mM EDTA and 0.75 M NaCl in 50 mM phosphate buffer pH 7.4), 5x Denhardt's solution, 0.5% (w/v) SDS, 100 µg/mL of denaturated heterologous DNA (salmon sperm DNA) and 30% (v/v) formamide. The membrane was washed two times in 2x SSC (0.3 M NaCl in 30 mM sodium citrate pH 7.0), 0.1% (w/v) SDS at room temperature for 10 min and once in 1x SSC, 0.1% SDS at 65°C for 15 min. The probe (SMA1 cDNA) was radiolabeled by nick translation using [α -³²P]dCTP (Amersham).

Sarcoplasmic reticulum preparation – The sarcoplasmic reticulum (SR), prepared from rabbit skeletal muscle using the method described in [29], was resuspended at a concentration of 20 mg/mL of protein, in 100 mM KCl, 10% (w/v) sucrose, 20 mM MOPS/KOH, pH 6.8 and stored in liquid nitrogen.

Subcellular fractionation – After an overnight culture in selective minimal dropout medium, cells at a density of 20-30x10⁶ cells/mL were collected by centrifugation (4°C/4,000xg/5 min) and washed twice with cold deionized water. After resuspension in 250 mM sorbitol, 1 mM MgCl₂, 10 mM imidazole, pH 7.5, (medium A), cells were broken with glass beads. The lysate was centrifuged (4°C/1,000xg/5 min) to remove debris and unbroken cells. The supernatant (crude homogenate) was centrifuged (4°C/15,000xg/40 min), yielding the P₁₅ pellet (membrane fraction). The P₁₅ pellet was resuspended in medium A, homogenized by potterisation, quickly frozen in liquid nitrogen and stored at -80°C. Protein concentration was determined using the Pierce™ BCA Protein Assay Kit (Thermo Scientific).

Western analysis - Proteins precipitated following the procedure described in [30] were separated by SDS-PAGE and transferred to nitrocellulose membrane by standard procedures. SMA1 was detected in the P₁₅ fraction using polyclonal antiserum raised against the purified reticulum sarcoplasmic Ca²⁺-ATPase SERCA1a [31], revealed using ¹²⁵I-labelled protein A. The monoclonal antibody MA3-912 was purchased from Invitrogen.

ATPase activity measurement - ATPase activity was measured at 25°C in 1080 µL of 50 mM MOPS, 50 mM MES, 50 mM TRIS-HCl, pH 7, 100 mM KCl, 1 mM MgCl₂, 10 µM A23187 (calcium ionophore), containing 240 µg of the P₁₅ pellet. A23187 is commonly used on SR to limit free Ca²⁺ accumulation inside vesicles, an accumulation that would prevent Ca²⁺ release from SERCA1a and thereby would inhibit its ATPase activity. To avoid such an inhibition, we added A23187 in our assays

on the P₁₅ pellet. For the “blank”, 180 µL of the reaction medium were first mixed to 50 µL of ice-cold 0.33 N HCl followed by the addition of 20 µL of 10 µM ATP. On the remaining sample (900 µL), the enzymatic reaction was initiated by addition of 100 µL of 10 µM ATP (pH 6.8) and stopped 20, 40, 60 and 80 s later by mixing 180 µL of the reaction medium to 50 µL of cold 0.33 N HCl. Samples were incubated 30 min in ice, centrifuged 10 min at 13000 rpm (Micro Centaur centrifuge MSE) and 200 µL of the supernatant were then neutralized by 100 µL of 0.2 M KOH. ATP content of each neutralized sample was measured by a luminescent method using the LKB Wallac Kit, in a reaction medium containing 600 µL of 250 mM TRIS, 5 mM EDTA, 17 mM potassium acetate pH 7.75, and 50 µL of Luciferin/Luciferase mix (prepared following LKB instructions). Each sample was treated in three steps as follows: first, 10 µL of 0.1 µM ATP were mixed to the reaction medium so as to obtain an internal calibration of the luminescent reaction. This was followed by 3 successive additions of 10 µL of the sample, and once more 10 µL of 0.1 µM ATP to check the stability of the response. The linearity of the luminescent method in our experimental conditions was tested from 5×10^{-13} to 1.2×10^{-11} mole of ATP. The way of preparation of our samples (acid quenching followed by neutralization) does not give any observable ATP degradation.

Phosphorylation assays – Phosphorylation assays from ATP were carried out at 0°C in 0.2 mL of 20 mM MOPS-KOH, pH 7.0, 80 mM KCl, 5 mM MgCl₂, 10 µM calcium ionophore A23187 supplemented with either EGTA, TG, orthovanadate or various CaCl₂ concentrations as indicated in the figure legends. Phosphorylation reaction was started by the addition of 1 µM [γ -³²P]-ATP (50–500 µCi.nmol⁻¹) and stopped 10 s later by the addition of 1 mL of ice-cold 7% (w/v) trichloroacetic acid (TCA), 1 mM KH₂PO₄. Precipitated proteins were collected by centrifugation, washed twice with 1 mL of ice cold 7% (w/v) TCA, 1 mM KH₂PO₄ and analyzed by acidic SDS-PAGE. After electrophoresis, the gel was dried and exposed to Kodak X-Omat AR5 film at -70°C.

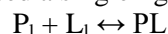
Phosphorylation assays from Pi were carried out at 25°C in 100 µL of 50 mM MES/TRIS pH 6.0, 5 mM MgCl₂, 10 µM calcium ionophore A23187, 20% (v/v) dimethyl sulfoxide, supplemented with 2 mM EGTA or 100 µM CaCl₂. The phosphorylation reaction was initiated by addition of 500 µM ³²Pi (10–100 µCi.nmol⁻¹) to the reaction mixture. After 10 min, the reaction was stopped by addition of 1 mL of ice-cold 7% TCA (w/v), 1 mM KH₂PO₄ and the samples were treated as described for the phosphorylation from ATP.

For quantitative analyses of the phosphorylation from ATP, samples were filtered on a GFF glass microfiber filter (Whatman). Filters were later washed with 6x5 mL of 30 mM KH₂PO₄, 1 mM ATP, 10% (w/v) TCA and were dissolved in 7.5 mL of scintillation liquid (Cytosint™, ICN). The radioactivity was measured on the TRI-CARB2100TR scintillation spectrometer (Packard Instrument Company).

Electron microscopy and immunodecoration - were performed as described in [32]. SMA1 was detected using polyclonal antiserum raised against the purified reticulum sarcoplasmic Ca²⁺-ATPase SERCA1a [31] coupled to a ProteinA gold (10 nm) conjugate.

Sequence analyses – *S. mansoni* sequences were taken from GeneDB (<http://www.genedb.org>). Exons search were made using ExPaSY Translate tools (<https://www.expasy.org/>). Sequences of the 102 Ca²⁺-ATPases referred in Table S1 were aligned with Clustal Omega Multiple Sequence Alignment [33].

Data fitting – Data were fitted using the standard Hill equation except in the particular case of the inhibition of SERCA1a by TG, where we used a single ligand binding model described below.



P₁ : free protein; L₁ : free ligand; PL : protein-ligand complex

The concentration of PL ([PL]) is obtained by the resolution of the following equation where K is the adjustable variable:

$$[PL]^2 - [PL](p+l+K) + pl = 0$$

p : total protein concentration ; l : total ligand concentration ; K : dissociation constant

RESULTS

In their study published in 2012, Altshuler and collaborators had identified *S. mansoni* as the only invertebrate with two SERCA-type Ca^{2+} -ATPases, SMA1 and SMA2 [23]. In a preamble of the present work, we analyzed the recent genomic data available at WormBase ParaSite (<http://parasite.wormbase.org>) to know whether the presence of two SERCA pumps was actually a particularity of *S. mansoni*. This analysis that we focused on Platyhelminthes (flatworms) revealed that other schistosomes like *S. japonicum*, *S. matthei* and *S. rodhaini* had orthologs of SMA1 and SMA2. We also found them in parasites of different families like *Echinococcus granulosus*, *Hymenolepis nana*, *Fasciola hepatica*, *Gyrodactylus salaris*, *Schistocephalus solidus* and *taenia asiatica*. To address the question of SERCA pumps redundancy in flatworms, we compared SMA1 and SMA2 at gene, protein transcriptomic but also enzymatic levels.

Similarity between SMA1 and SMA2 at the gene and protein levels - The architectures of *SMA1* and *SMA2* genes are very similar. Indeed, eleven of the sixteen exons of *SMA1* have their counterpart in *SMA2*. The three differences between the two genes are on the one hand the splitting of *SMA1* exon 2 in two exons in *SMA2* (exons 2+3) and on the other hand the fusion of exons (5+6) and (9+10) of *SMA1* into unique exons in *SMA2* (exons 6 and 9) (Fig. 1A). Overall, the coding sequences of *SMA1* and *SMA2* display 65% identity. Together, these observations strongly suggests that the presence of *SMA1* and *SMA2* might be the result of a duplication event.

At the protein level, we first compared SMA1 and SMA2 to 102 sequences of Ca^{2+} -ATPases of various origins. Plasma Membrane Ca^{2+} -ATPases which obviously constitute a distinct subfamily of Ca^{2+} -ATPases were excluded from the comparison. As shown in Fig 1B, SMA1 displays 60 to 65 % identity with SERCA-type Ca^{2+} -ATPases and Ca^{2+} -ATPases of various eukaryotic non-vertebrate organisms like insects, crustaceans, nematodes, worms, mollusks, and parasites. It displays only 40 to 50% identity with plants and algae Ca^{2+} -ATPases and 20 to 30% identity with fungi, bacteria and Secretory Pathway Ca^{2+} -ATPases (SPCA). Note that SMA1 exhibits 85% identity with Sjp1, its ortholog in *Schistosoma japonicum*. A similar profile is found for SMA2 (which also possesses an ortholog in *S. japonicum*, sjp2) at the exception of a slightly higher identity to SERCA pumps. SMA3 obviously differs from SMA1 and SMA2 and rather classifies in a group comprising fungal and SPCA-type Ca^{2+} -ATPases.

Concerning the proteins compared in the present study, SMA1 displays 64% and 66% identity (77% and 79% similarity) with SERCA1a (the rabbit SR Ca^{2+} -ATPase) and SMA2, respectively. Notably, SMA1 possesses all the amino acids identified in SERCA1a as constituting the two Ca^{2+} -binding sites: Asn⁷⁷⁰, Glu⁷⁷³, Thr⁸⁰¹ and Glu⁹¹⁰ for site I; Val³⁰⁵, Ala³⁰⁶, Ile³⁰⁸ (which contribute by their main chain oxygen), Glu³¹⁰ and Asn⁷⁹⁸ for site II; Asp⁸⁰¹ shared by the two sites. A schematic representation shows two highly identical regions in the three ATPases, one extending from Tm4 to the first part of the P domain, another one extending from the end of the P domain to Tm9. The less conserved region between the three pumps is obviously the nucleotide binding N domain (Fig 1C).

Phospholamban (PLN) is a 52-amino acid membrane protein which inhibits SERCA1 and SERCA2 but not SERCA3 isoforms [21]. On the basis of the PLN-SERCA1a interaction model [34], we analyzed the sequence of SMA1 and found that 21 of the 25 amino acids of the PLN binding pocket of SERCA1a were present in SMA1. Contrary to what has been previously published [21], SMA2 also displays a PLN-binding site.

In vertebrates, SERCA isoforms differ by their location (SERCA1 in skeletal muscle, SERCA2 in smooth muscle and SERCA3 in non-muscle cells) and by their distribution during development (fetal vs adult). They also differ by some enzymatic characteristics such as their affinity for Ca^{2+} [35] and their sensitivity to specific inhibitors like TG and CPA [36]. In the present work, we chose these criteria to compare SMA1 and SMA2. In order to make the comparison relevant, we used for the production of SMA1, the same expression system as that used for SMA2, the yeast *S. cerevisiae* [21]. We also took the same reference, namely SERCA1a, which we experimentally tested in the same conditions as those used for SMA1.

Expression of SMA1 in yeast - The constitutive expression of *SMA1* in *S. cerevisiae* was carried out from the multicopy YEp195SMA1 vector and was detected at the transcription level by Northern blot. As shown in Fig 2A, *SMA1* transcript displays the expected size of about 3.5 kb, comprising the 3069 nt of *SMA1*, the 233 nt from the 5' non-coding region of the *PMA1* promoter [37] and about 200 nucleotides from the 3' "polyA" region.

To detect the SMA1 protein in the yeast membrane extract (P₁₅ fraction), we used a polyclonal antibody raised against SERCA1a [31]. As previously published [38] and shown here in Fig 2B, this antibody efficiently detects SERCA1a in the P₁₅ fraction of a strain transformed with the YEp195PSA vector. In this fraction, a small part of SERCA1a appears as oligomers of higher molecular weights and as a band of about 80 kDa which probably comes from a slight proteolysis. In the P₁₅ fraction of a strain transformed with the YEp195SMA1 vector, the polyclonal antibody specifically recognizes a protein of the size expected for SMA1. SMA1 shows no degradation and displays oligomeric forms of sizes similar to those observed for SERCA1a. Note that the polyclonal antibody also cross reacts with an endogenous yeast protein of 50 kDa present in all P₁₅ fractions. To detect SMA1 in yeast membranes, we also tested the monoclonal antibody MA3-912, which recognizes an epitope located between the residue 506 and the C-terminus of SERCA1a. Although successfully used to detect SERCA1 ATPases in many vertebrates, this antibody was found unable to detect SMA1 (data not shown). Finally, as judged by their respective intensities, SMA1 and SERCA1a are produced at the same level in yeast, estimated to about 0.5 to 1 mg per liter of culture (about 1 % (w/w) of the protein content of the P₁₅ fraction).

SMA1 accumulates in particular internal membranes in S. cerevisiae - Electron microscopy revealed that yeast cells producing SMA1 exhibited two types of internal membranes proliferations derived from endoplasmic reticulum, PER and Karmellae. PER for Proliferating Endoplasmic Reticulum, consist of amorphous membrane structures, initially described in a yeast strain overexpressing PMA2, one of the two yeast H⁺-ATPases [32] and later in a yeast strain expressing SERCA1a [38]. Karmellae consist of long pieces of regularly stacked membranes observed in yeast cells expressing the H⁺-ATPase PMA2 of the plant *Nicotiana plumbaginifolia* [39]. In the case of SMA1, these two membrane proliferations, induced by the expression process, are sometimes found in the same cell (Fig 3A). SMA1 almost exclusively accumulates in these two membrane networks as illustrated with Karmellae (Fig 3B).

In the two next sections, SMA1 activity in yeast membranes will be assessed by ATPase activity and phosphorylation assays. Phosphorylation from ATP will be used in the two last sections to measure SMA1 apparent affinity for Ca²⁺ and to characterize the inhibitory effects of TG and CPA.

ATPase activity of SMA1 in yeast membranes - If SMA1 is active and in sufficient amount in yeast membranes, its ATPase activity should be detected provided that the reaction conditions and the method are correctly chosen. In terms of reaction conditions, two parameters were found critical, pH and ATP concentration. pH was adjusted to 7, the optimum pH of SERCA1a (and presumably SMA1) but 1 order of magnitude higher than the optimum pH of the plasma membrane H⁺-ATPase (naturally enriched in the P₁₅ fraction) and 2 orders of magnitude lower than the optimal pH of the mitochondrial ATPase [40]. ATP concentration was adjusted to 1 μM, close to the K_m of SERCA1a [41] (and presumably SMA1) but about 200 times lower than the K_m of the vacuolar H⁺-ATPase [42] and 3 orders of magnitude lower than the K_m of the plasma membrane and the mitochondrial ATPases. In terms of method, we used a luciferin/luciferase ATP detection assay. This very sensitive method allowed us to measure ATPase activities ranging from 1 to 5 nmoles of ATP hydrolyzed per min and mg of total protein, in the P₁₅ fractions of non-expressing (NE-) and expressing (E-) strains. Finally, to discriminate between endogenous ATPases and SMA1, we compared the effects of two well-known inhibitors of P-type ATPases, vanadate and TG, in the presence of 100 μM CaCl₂. TG is a specific inhibitor of SERCA pumps whereas vanadate is an analogue of phosphate that inhibits rather non-specifically a large number of ATP-utilizing enzymes among them P-type ATPases [36]. If SMA1 activity is high enough, the relative inhibitory effect of these two compounds should be stronger on the ATPase activity of the P₁₅ fraction containing the schistosomal Ca²⁺-ATPase than of the P₁₅ fraction of the NE-strain.

As shown in Fig 4A, a TG-sensitive ATPase activity accounting for about one third of the total ATPase activity is detected in the P₁₅ fraction of the E-strain. As expected, no TG-sensitive ATPase activity is detected in the P₁₅ fraction of the NE-strain, what can be explained by the absence of SERCA pumps in yeast and by the low abundance and the low sensitivity to TG of Pmr1p, the SPCA pump of *S. cerevisiae* [43]. The presence of an additional P-type ATPase activity in the E-strain was confirmed by a more pronounced inhibitory effect of vanadate: the remaining activity in the P₁₅ fraction of the E-strain represents about 48% of the total ATPase activity versus about 72% in the NE-strain. Together, these results strongly suggest the presence of active SMA1 in the P₁₅ fraction of the E-strain.

SMA1 phosphorylation from ATP and Pi - A remarkable property of P-type ATPases is their ability to be phosphorylated on a conserved aspartate residue located in the P-domain. This phosphorylation can be achieved in two different ways. The forward phosphorylation consists in the transfer of the γ phosphate of ATP to the carboxyl group of the aspartate residue and only occurs in the presence of the transported ion. This phosphorylation also called “forward” phosphorylation is transient and coupled to ion transport. The backward phosphorylation is the covalent binding of inorganic phosphate to the carboxyl group of the aspartate residue and only occurs in the absence of the transported ion. On SERCA1a, the phosphorylation from Pi is strongly improved by the addition of 10-20% (v/v) dimethyl sulfoxide and the absence of potassium.

As shown in Fig 4B, a phosphorylated band of the size expected for SMA1, is observed in the P₁₅ fraction of the E-strain, when a phosphorylation assay from 1 μ M radioactive [γ -³²P]ATP is carried out in the presence of 1 μ M free calcium. This band almost totally disappears upon addition of 100 μ M EGTA, a divalent ion chelator, and is absent in the P₁₅ fraction of the NE-strain. It is also absent in the P₁₅ fraction of the strain expressing the D354A mutant (akt) in which the aspartate residue phosphorylated during the catalytic cycle of SMA1 has been replaced by an alanine. As expected SMA1 phosphorylation from ATP depends on calcium concentration and is totally inhibited by 50 μ M TG (Fig 4C). Note that a phosphorylated band of weak intensity and insensitive to EGTA and TG, is observed in the P₁₅ fractions of E- and NE- strains. Fig 4D shows that SMA1 can also be phosphorylated from Pi in the absence of free calcium i.e. in the presence of 2 mM EGTA. As control, the two types of phosphorylation have been carried out on SERCA1a in the same experimental conditions as those used for SMA1 (Fig 4C and 4D). Note that in both experiences, the phosphorylation intensities roughly correlate with the expected amount of SMA1 and SERCA1a (assuming that SMA1 represents 0.5 to 1% (w/w) of the proteins in the P₁₅ pellet and that SERCA1a represents about 80% (w/w) of SR proteins). These experiments which confirm that SMA1 produced in *S. cerevisiae* is active, show that it also displays phosphorylation properties of SERCA pumps.

Taking advantage of the low phosphorylation background seen on acidic gels (Fig 4B and 4C), we applied on yeast membranes, a filtration method usually used to measure SERCA1a phosphorylation on the purified sarcoplasmic reticulum. To quantify the contribution of SMA1, we compared the phosphorylation intensities in the E- versus the NE- strain, in the presence of 100 μ M CaCl₂, 2 mM EGTA or 100 μ M CaCl₂ plus 50 μ M TG. As shown in Fig 5A, a TG and EGTA sensitive phosphorylation accounting for more than 60% of the total phosphorylation and attributable to SMA1 was measured in the P₁₅ fraction of the E-strain. Almost no variation of the phosphorylation intensity was measured in the P₁₅ fraction of the NE-strain. As expected, phosphorylation of SERCA1a in the purified sarcoplasmic reticulum (SR) is almost totally inhibited in the presence of EGTA or TG.

SMA1 apparent affinities for Ca²⁺ - It is well known on SERCA1a that phosphorylation from ATP is not inhibited at high calcium concentration and can therefore be used to determine the apparent affinity for the transported ion [44]. As shown in Fig 5B, SERCA1a phosphorylation from ATP and that of SMA1 display the same dependency to free calcium concentration characterized by apparent K_d of 0.41 +/- 0.04 μ M for SERCA1a and 0.45 +/- 0.06 μ M for SMA1. In addition, SERCA1a and SMA1 both display a Hill coefficient around 1.3, consistent with a positive cooperativity of calcium binding.

SMA1 inhibition by TG and CPA - As shown in Fig 5C, SERCA1a and SMA1 are strongly inhibited by TG. SERCA1a inhibition is observed in a narrow range of TG concentration (about one decade) and is almost achieved at 10^{-7} M, a concentration close to that of SERCA1a in the assay estimated at 0.91×10^{-7} M (SERCA1a molecular weight: 109489 Da; SERCA1a concentration in the assay: 10 $\mu\text{g/mL}$). Taking into account SERCA1a concentration in the assay and applying a single ligand binding model, we estimated an apparent K_i of 12 ± 0.36 nM in our experimental conditions. Note that the shape of this curve strongly suggests that it corresponds to a titration of SERCA1a by TG (see discussion).

Assuming that SMA1 represents about 1% (w/w) of the proteins present in the P_{15} fraction of the E-strain, its concentration wouldn't exceed 2.2×10^{-8} M in the assay (SMA1 molecular weight: 112594 Da; 250 $\mu\text{g/mL}$ of P_{15} fraction in the assay). SMA1 inhibition by TG obviously does not correspond to a titration and was well fitted with a standard Hill equation (considering one binding site), giving an apparent K_i of 26.3 ± 5.1 nM.

As expected, higher concentrations of CPA are required to inhibit SERCA1a and SMA1 (Fig 5D). For SERCA1a, we used a Hill equation to calculate an apparent K_i of 1.2 ± 0.3 μM , considering one binding site of CPA per protein. For SMA1, the inhibition by CPA extends over more than 2 decades (10^{-7} to more than 10^{-4}) which does obviously not reflect the sole binding of one CPA per SMA1. This might be explained by the fact that SMA1 only accounting for about 1% of the total protein content of the P_{15} fraction, a significant amount of CPA might interact with other ligands in yeast membranes (by comparison SERCA1a is almost the only protein present in the SR). Thereby, the apparent K_i of SMA1 is probably lower than the value of 9.8 ± 1.6 μM obtained by fitting the data with a standard Hill equation.

DISCUSSION

As shown in the first part of this manuscript, SMA1 and SMA2 are very close in terms of gene and protein sequence. In order to compare their enzymatic properties, we produced SMA1 in *S. cerevisiae*, the expression system previously used for SMA2. By optimizing experimental conditions, we were able to measure SMA1 ATPase activity and SMA1 phosphorylation in yeast membranes. This led us to characterize the binding of calcium to SMA1 as well as the sensitivity of SMA1 to TG and CPA. In the following, these data will be compared to those previously obtained on SMA2.

In mammals, the three types of SERCA pumps bind two calcium ions in a cooperative manner [45] but SERCA1 and SERCA2 present in muscle cells have slightly better affinities for calcium than SERCA3 present in non-muscle cells, (apparent K_d around 0.4 μM for the former, 1.1 μM for the latter). Regarding these two criteria, SMA1, with an apparent K_d for calcium of 0.4 μM and a Hill number of 1.3, is closer to muscle than non-muscle cells Ca^{2+} -ATPases. This is also the case of SMA2 for which an apparent K_d of 1 μM and a Hill coefficient of 1.29 have been determined in the past [21].

Another functional characteristic specific of SERCA1 and SERCA2 is their regulation by PLN. In our analysis, we found a PLN binding site in SMA1 located in a groove formed by Tm2, Tm4, Tm6 and Tm9. We also found a PLN binding site in SMA2, contrary to what has been previously published. To go further, we searched in the *S. mansoni* genome a gene coding for PLN and for that we used as probes different sequences classified in the PF04272 Pfam family. Surprisingly, none of these probes allowed us to find a PLN gene in *S. mansoni* genome.

TG specifically inhibits SERCA pumps by stabilizing the non-phosphorylated calcium-free state. In their pioneer work, Sagara and collaborators [46] showed that TG inhibited SERCA1a by a stoichiometric titration at concentrations as low as nanomolar but later, several studies tried to accurately assess the sensitivity to TG of SERCA isoforms expressed in different cell lines. In COS-1 cells, a same IC_{50} of 0.15 nM was found for SERCA1, SERCA2a and SERCA2b isoforms, by measurements of the initial rates of calcium uptake [47]. In contrast, in COS-7 cells, ATPase activity measurements evidenced isoforms-specific inhibitory effects of TG with apparent K_i varying from 0.2 nM for SERCA1b to 1.3 nM for SERCA2b and 12 nM for SERCA3a [48]. The differences between

these two studies highlight the difficulty to compare TG efficiencies from different experimental conditions and different types of measurement.

In the present study, we measured the sensitivity of SMA1 and SERCA1 to TG in the same experimental conditions and found that the two pumps were very close to one another. It is also important to note that the inhibition curve obtained in our conditions for SERCA1a is comparable to that previously obtained at the same concentration of the protein by ATPases activity and calcium transport assays [46]. The result concerning SMA1 was expected since it possesses almost all the residues in Tm3, Tm5 and Tm7 constituting the TG binding pocket of SERCA1a. The only two differences are the conservative replacements of Leu²⁵³ and Val⁷⁶⁹ in the TG binding pocket of SERCA1a by Ile²⁵⁴ and Ile⁷⁷¹ in SMA1, respectively (Table S2). SMA2 sensitivity to TG, characterized by an IC₅₀ of 18.1 μM [21], strongly differs from that of SERCA1a and SMA1. As suggested by the authors, this low sensitivity could be linked to the use of detergent during the preparation of yeast membrane fractions enriched in SMA2. However, it could also reflect an intrinsic property of SMA2. Indeed, the TG binding pockets of SMA2 and SERCA1a exhibit two differences. One is the conservative replacement of Val⁷⁶⁹ in SERCA1a by Ile⁷⁷⁸ in SMA2 but the other is the non-conservative replacement of Met⁸³⁸ in SERCA1a by Val⁸⁴⁷ in SMA2 (Table S2). It is obviously not possible to say that the absence of a methionine residue in the TG binding pocket of SMA2 explains by itself its low sensitivity to the drug but interestingly, the Ca²⁺-ATPase PfATP6, which has a low sensitivity to TG (IC₅₀ >150 μM), displays three non-conservative replacements compared to SERCA1a among them, the replacement of Met⁸³⁸ by Ile¹⁰⁴⁹ [49]. In addition, non-conservative changes at the position corresponding to Met⁸³⁸ in SERCA1a are also found in SERCA2 (Leu⁸³⁷) and SERCA3 (Leu⁸³⁸) (Table S2).

CPA which binds in a groove formed by Tm1, Tm2 Tm3 and Tm4 [36] is a less potent inhibitor of SERCA pumps than TG, with apparent Ki of 90 nM for SERCA1b, 2.5 μM for SERCA2b and 0.6 μM for SERCA3a, determined by ATPase activity measurements [48]. In the present study, we found an apparent Ki for SMA1 very similar to that previously measured for SMA2 [21]. However, as explained above, the apparent Ki values for SMA1 and SMA2 are probably overestimated due to the binding of CPA to other ligands in yeast membranes. The similar behavior of SMA1, SMA2 and SERCA1a to CPA exposure was expected given the strong similarity between the CPA binding pockets of the three ATPases. Indeed, the CPA binding pockets of SERCA1a and SMA2 are identical and only differ from that of SMA1a by one conservative replacement (Leu²⁵³ in SERCA1a replaced by Ile²⁵⁴ in SMA1) (Table S2).

Our study did not reveal major functional differences between SMA1 and SMA2, except their sensitivity to TG. To know whether the presence of two SERCA pumps in *S. mansoni* might be explained by requirements at particular stages of parasite development, we looked at transcriptomic data available at GeneDB and obtained for four parasite forms: the free-living cercariae, the 3- and 24-hours schistosomula (S3H and S24H) and the adult worm (A) [20]. This analysis revealed that *SMA1* and *SMA2* had different expression profiles during parasite development (Fig. S1). *SMA1* expression gradually increases from the cercariae to the adult worm. In parallel, *SMA2* expression strongly decreases during the cercariae to schistosomula transition but strongly increases during the schistosomula to adult worm transition. This might reflect distinct roles of the two SERCA pumps: SMA1 would ensure basal muscular functions whereas SMA2 would be specifically expressed in particular organs and required at specific development stages of the parasite. Our hypothesis is that SMA2 might be essential for muscle contractibility of the bifurcated tail, the organ that allows cercariae to swim and which is lost when cercariae transforms into schistosomula, the transition during which *SMA2* expression dramatically falls down. So far, the localization of SMA1 and SMA2 in the different forms of the parasite are not known but would be required to validate this hypothesis.

ACKNOWLEDGMENTS

This study received the financial support of the Commissariat à l'Énergie Atomique et aux Énergies Alternatives. We thank A. Goffeau for the critical reading of the manuscript

REFERENCES

1. Jencks WP (1989) Utilization of binding energy and coupling rules for active transport and other coupled vectorial processes. *Methods Enzymol* 171: 145-164.
2. Bublitz M, Poulsen H, Morth JP, Nissen P (2010) In and out of the cation pumps: P-type ATPase structure revisited. *Curr Opin Struct Biol* 20: 431-439.
3. Kenthirapalan S, Waters AP, Matuschewski K, Kooij TW (2014) Copper-transporting ATPase is important for malaria parasite fertility. *Mol Microbiol* 91: 315-325.
4. Krishna S, Pulcini S, Moore CM, Teo BH, Staines HM (2014) Pumped up: reflections on PfATP6 as the target for artemisinins. *Trends Pharmacol Sci* 35: 4-11.
5. Spillman NJ, Kirk K (2015) The malaria parasite cation ATPase PfATP4 and its role in the mechanism of action of a new arsenal of antimalarial drugs. *Int J Parasitol Drugs Drug Resist* 5: 149-162.
6. Coelho AC, Boisvert S, Mukherjee A, Leprohon P, Corbeil J, et al. (2012) Multiple mutations in heterogeneous miltefosine-resistant *Leishmania major* population as determined by whole genome sequencing. *PLoS Negl Trop Dis* 6: e1512.
7. de Almeida-Amaral EE, Caruso-Neves C, Pires VM, Meyer-Fernandes JR (2008) *Leishmania amazonensis*: characterization of an ouabain-insensitive Na⁺-ATPase activity. *Exp Parasitol* 118: 165-171.
8. Rastew E, Vicente JB, Singh U (2012) Oxidative stress resistance genes contribute to the pathogenic potential of the anaerobic protozoan parasite, *Entamoeba histolytica*. *Int J Parasitol* 42: 1007-1015.
9. Iizumi K, Mikami Y, Hashimoto M, Nara T, Hara Y, et al. (2006) Molecular cloning and characterization of ouabain-insensitive Na⁽⁺⁾-ATPase in the parasitic protist, *Trypanosoma cruzi*. *Biochim Biophys Acta* 1758: 738-746.
10. Colley DG, Bustinduy AL, Secor WE, King CH (2014) Human schistosomiasis. *Lancet* 383: 2253-2264.
11. Noel F, Soares de Moura R (1986) *Schistosoma mansoni*: preparation, characterization of (Na⁺ + K⁺)ATPase from tegument and carcass. *Exp Parasitol* 62: 298-307.
12. Braschi S, Curwen RS, Ashton PD, Verjovski-Almeida S, Wilson A (2006) The tegument surface membranes of the human blood parasite *Schistosoma mansoni*: a proteomic analysis after differential extraction. *Proteomics* 6: 1471-1482.
13. Da'dara AA, Faghiri Z, Krautz-Peterson G, Bhardwaj R, Skelly PJ (2013) Schistosome Na,K-ATPase as a therapeutic target. *Trans R Soc Trop Med Hyg* 107: 74-82.
14. Skelly PJ, Dougan PM, Maule A, Day TA, Shoemaker CB (2001) Cloning and characterization of a muscle isoform of a Na,K-ATPase alpha subunit (SNaK1) from *Schistosoma mansoni*. *Parasitology* 123: 277-284.
15. Cunha VM, de Souza W, Noel F (1988) A Ca²⁺-stimulated, Mg²⁺-dependent ATPase activity in subcellular fractions from *Schistosoma mansoni*. *FEBS Lett* 241: 65-68.
16. Cunha VM, Meyer-Fernandes JR, Noel F (1992) A (Ca²⁺)-Mg²⁺ATPase from *Schistosoma mansoni* is coupled to an active transport of calcium. *Mol Biochem Parasitol* 52: 167-173.
17. Cunha VM, Noel F (1998) (Ca²⁺)-Mg²⁺ATPase in *Schistosoma mansoni*: evidence for heterogeneity and resistance to praziquantel. *Mem Inst Oswaldo Cruz* 93 Suppl 1: 181-182.
18. de Mendonca RL, Beck E, Rumjanek FD, Goffeau A (1995) Cloning and characterization of a putative calcium-transporting ATPase gene from *Schistosoma mansoni*. *Mol Biochem Parasitol* 72: 129-139.
19. Berriman M, Haas BJ, LoVerde PT, Wilson RA, Dillon GP, et al. (2009) The genome of the blood fluke *Schistosoma mansoni*. *Nature* 460: 352-358.
20. Protasio AV, Tsai IJ, Babbage A, Nichol S, Hunt M, et al. (2012) A systematically improved high quality genome and transcriptome of the human blood fluke *Schistosoma mansoni*. *PLoS Negl Trop Dis* 6: e1455.
21. Talla E, de Mendonca RL, Degand I, Goffeau A, Ghislain M (1998) *Schistosoma mansoni* Ca²⁺-ATPase SMA2 restores viability to yeast Ca²⁺-ATPase-deficient strains and functions in calcineurin-mediated Ca²⁺ tolerance. *J Biol Chem* 273: 27831-27840.

22. Da'dara A, Tsai MH, Tao LF, Marx KA, Shoemaker CB, et al. (2001) Schistosoma mansoni: molecular characterization of a tegumental Ca-ATPase (SMA3). *Exp Parasitol* 98: 215-222.
23. Altshuler I, Vaillant JJ, Xu S, Cristescu ME (2012) The evolutionary history of sarco(endo)plasmic calcium ATPase (SERCA). *PLoS One* 7: e52617.
24. Sikorski RS, Hieter P (1989) A system of shuttle vectors and yeast host strains designed for efficient manipulation of DNA in *Saccharomyces cerevisiae*. *Genetics* 122: 19-27.
25. Kuo C, Nuang H, Campbell JL (1983) Isolation of yeast DNA replication mutants in permeabilized cells. *Proc Natl Acad Sci U S A* 80: 6465-6469.
26. Gietz RD, Sugino A (1988) New yeast-*Escherichia coli* shuttle vectors constructed with in vitro mutagenized yeast genes lacking six-base pair restriction sites. *Gene* 74: 527-534.
27. Durr G, Strayle J, Plemper R, Elbs S, Klee SK, et al. (1998) The medial-Golgi ion pump Pmr1 supplies the yeast secretory pathway with Ca²⁺ and Mn²⁺ required for glycosylation, sorting, and endoplasmic reticulum-associated protein degradation. *Mol Biol Cell* 9: 1149-1162.
28. Schmitt ME, Brown TA, Trumpower BL (1990) A rapid and simple method for preparation of RNA from *Saccharomyces cerevisiae*. *Nucleic Acids Res* 18: 3091-3092.
29. Dupont Y (1977) Kinetics and regulation of sarcoplasmic reticulum ATPase. *Eur J Biochem* 72: 185-190.
30. Wessel D, Flugge UI (1984) A method for the quantitative recovery of protein in dilute solution in the presence of detergents and lipids. *Anal Biochem* 138: 141-143.
31. Enouf J, Lompre AM, Bredoux R, Bourdeau N, de La Bastie D, et al. (1988) Different sensitivity to trypsin of the human platelet plasma and intracellular membrane Ca²⁺ pumps. *J Biol Chem* 263: 13922-13929.
32. Supply P, Wach A, Thines-Sempoux D, Goffeau A (1993) Proliferation of intracellular structures upon overexpression of the PMA2 ATPase in *Saccharomyces cerevisiae*. *J Biol Chem* 268: 19744-19752.
33. Sievers F, Wilm A, Dineen D, Gibson TJ, Karplus K, et al. (2011) Fast, scalable generation of high-quality protein multiple sequence alignments using Clustal Omega. *Mol Syst Biol* 7: 539.
34. Toyoshima C, Asahi M, Sugita Y, Khanna R, Tsuda T, et al. (2003) Modeling of the inhibitory interaction of phospholamban with the Ca²⁺ ATPase. *Proc Natl Acad Sci U S A* 100: 467-472.
35. Periasamy M, Kalyanasundaram A (2007) SERCA pump isoforms: their role in calcium transport and disease. *Muscle Nerve* 35: 430-442.
36. Michelangeli F, East JM (2011) A diversity of SERCA Ca²⁺ pump inhibitors. *Biochem Soc Trans* 39: 789-797.
37. Capieaux E, Vignais ML, Sentenac A, Goffeau A (1989) The yeast H⁺-ATPase gene is controlled by the promoter binding factor TUF. *J Biol Chem* 264: 7437-7446.
38. Degand I, Catty P, Talla E, Thines-Sempoux D, de Kerchove d'Exaerde A, et al. (1999) Rabbit sarcoplasmic reticulum Ca(2+)-ATPase replaces yeast PMC1 and PMR1 Ca(2+)-ATPases for cell viability and calcineurin-dependent regulation of calcium tolerance. *Mol Microbiol* 31: 545-556.
39. de Kerchove d'Exaerde A, Supply P, Dufour JP, Bogaerts P, Thines D, et al. (1995) Functional complementation of a null mutation of the yeast *Saccharomyces cerevisiae* plasma membrane H(+)-ATPase by a plant H(+)-ATPase gene. *J Biol Chem* 270: 23828-23837.
40. Foury F, Amory A, Goffeau A (1981) Large-scale purification and phosphorylation of a detergent-treated adenosine triphosphatase complex from plasma membrane of *Saccharomyces cerevisiae*. *Eur J Biochem* 119: 395-400.
41. Lacapere JJ, Bennett N, Dupont Y, Guillain F (1990) pH and magnesium dependence of ATP binding to sarcoplasmic reticulum ATPase. Evidence that the catalytic ATP-binding site consists of two domains. *J Biol Chem* 265: 348-353.
42. Uchida E, Ohsumi Y, Anraku Y (1988) Purification of yeast vacuolar membrane H⁺-ATPase and enzymological discrimination of three ATP-driven proton pumps in *Saccharomyces cerevisiae*. *Methods Enzymol* 157: 544-562.
43. Sorin A, Rosas G, Rao R (1997) PMR1, a Ca²⁺-ATPase in yeast Golgi, has properties distinct from sarco/endoplasmic reticulum and plasma membrane calcium pumps. *J Biol Chem* 272: 9895-9901.

44. Andersen JP, Vilsen B (1998) Structure-function relationships of the calcium binding sites of the sarcoplasmic reticulum Ca(2+)-ATPase. *Acta Physiol Scand Suppl* 643: 45-54.
45. Lytton J, Westlin M, Burk SE, Shull GE, MacLennan DH (1992) Functional comparisons between isoforms of the sarcoplasmic or endoplasmic reticulum family of calcium pumps. *J Biol Chem* 267: 14483-14489.
46. Sagara Y, Inesi G (1991) Inhibition of the sarcoplasmic reticulum Ca²⁺ transport ATPase by thapsigargin at subnanomolar concentrations. *J Biol Chem* 266: 13503-13506.
47. Campbell AM, Kessler PD, Sagara Y, Inesi G, Fambrough DM (1991) Nucleotide sequences of avian cardiac and brain SR/ER Ca(2+)-ATPases and functional comparisons with fast twitch Ca(2+)-ATPase. Calcium affinities and inhibitor effects. *J Biol Chem* 266: 16050-16055.
48. Wootton LL, Michelangeli F (2006) The effects of the phenylalanine 256 to valine mutation on the sensitivity of sarcoplasmic/endoplasmic reticulum Ca²⁺ ATPase (SERCA) Ca²⁺ pump isoforms 1, 2, and 3 to thapsigargin and other inhibitors. *J Biol Chem* 281: 6970-6976.
49. Arnou B, Montigny C, Morth JP, Nissen P, Jaxel C, et al. (2011) The Plasmodium falciparum Ca(2+)-ATPase PfATP6: insensitive to artemisinin, but a potential drug target. *Biochem Soc Trans* 39: 823-831.
50. Schoenmakers TJ, Visser GJ, Flik G, Theuvenet AP (1992) CHELATOR: an improved method for computing metal ion concentrations in physiological solutions. *Biotechniques* 12: 870-874, 876-879.

FIGURE LEGENDS

Fig 1. A - Exons organization of *SMA1* and *SMA2*. Exons were identified by translation of *SMA1* and *SMA2*, using ExpASY Translate tool and positioned according to their corresponding amino acid sequence. **B** – Sequence identity (%) between the three schistosomal Ca²⁺-ATPases (*SMA1* (dark diamonds), *SMA2* (empty squares) and *SMA3* (grey triangles)) and 102 Ca²⁺-ATPases of various origins (listed in Table S1). **C** – Schematic representation of the identity between *SMA1*, *SMA2* and *SERCA1a*. Sequences were aligned with Clustal Omega. The identity at a given position was then converted using a home-made Excel macro, into a numerical value (1 when the same amino acid is found at the same position in the three sequences; 0 if not). The structural motifs of *SERCA1a* are schematized above. A-, N- and P-domains constitute the catalytic moiety of the transporter; Tm: transmembrane segment.

Fig 2. A – *SMA1* transcription. 20 µg of total RNA, extracted from yeast strains containing YEp195*SMA1* or YEp195PA (empty vector) were analyzed by Northern Blot. *SMA1* transcript was detected by autoradiography using a specific radiolabeled probe; ribosomal RNAs were detected by ethidium bromide staining. **B** – *SMA1* production. 10 and 20 µg of the P₁₅ fractions of yeast strains containing YEp195*SMA1*, YEp195PA or YEp195PSA (expressing *SERCA1a*) were precipitated and separated by SDS-PAGE. After blotting to nitrocellulose membrane, *SMA1* and *SERCA1a* (black arrow) were detected using a polyclonal antibody raised against *SERCA1a*.

Fig 3. A - Electron microscopy showing the two types of internal membrane proliferations induced by *SMA1* expression. PER: Proliferating Endoplasmic Reticulum; K: Karmellae; Nu: nucleus. Details of PER and Karmellae structures are shown on the left. The scale bar corresponds to 0.5 µm. **B** – Intracellular detection of *SMA1* by electron microscopy using a polyclonal antibody raised against *SERCA1a* and a Protein A gold conjugate. A cell containing Karmellae structures is shown with details of two regions. The scale bar corresponds to 0.5 µm.

Fig 4. A - ATPase activity was measured at 25°C using a luciferin/luciferase based chemiluminescent method on 240 µg of E- and NE- strains P₁₅ fractions, in a reaction medium containing 50 mM MOPS, 50 mM MES, 50 mM TRIS-HCl, pH 7, 100 mM KCl, 1 mM MgCl₂, 10 µM A23187, 100 µM CaCl₂ and 1 µM ATP. When indicated, TG and vanadate (Vn) were added at concentrations of 50 µM and 2.5 mM, respectively. The 100% value for each strain refers to the ATPase activity in the presence of 100 µM CaCl₂. Values are the average of 4 and 5 measurements for NE and E respectively, carried out

on 2 independent P₁₅ fractions of each strain. Student test gave the following P-values: < 0.01(***); 0.01 < P-value < 0.05 (**); 0.05 < P-value < 0.1 (*) **B** - Phosphorylation assays from [γ -³²P]ATP were carried out at 0°C, on 20 μ g of E- and NE- strains P₁₅ fractions as well as of the strain expressing the D354A mutant (akt), in a reaction medium containing 20 mM MOPS-KOH, pH 7.0, 80 mM KCl, 5 mM MgCl₂, 10 μ M A23187, in the presence of 100 μ M CaCl₂ (Ca) or 100 μ M EGTA. **C** - Phosphorylation assays from [γ -³²P]ATP were carried out as described above on 50 μ g of the E-strain P₁₅ fraction at three concentrations of free calcium (10⁻⁶, 10⁻⁷ and 10⁻⁸ M), or 2 mM EGTA or a mix containing 100 μ M CaCl₂ and 50 μ M TG. As control, phosphorylation assays were performed on 0,2 μ g of purified rabbit sarcoplasmic reticulum (SR) in the presence of 10⁻⁶ M free calcium or 2 mM EGTA. **D** - Phosphorylation assays from ³²Pi were performed at 25°C, on 24 μ g of the E-strain P₁₅ fraction and 0,4 μ g of SR, in a reaction medium containing 50 mM MES/TRIS pH 6.0, 5 mM MgCl₂, 10 μ M A23187, 20% (v/v) dimethyl sulfoxide supplemented with 2 mM EGTA or 100 μ M CaCl₂ (Ca).

Fig 5. Phosphorylation assays from [γ -³²P]ATP were carried out and quantified after filtration on GFF filters, on 250 μ g/mL of the P₁₅ fractions of E- and NE-strains or 10 μ g/ml of purified rabbit sarcoplasmic reticulum (SR) **A** – Reaction was performed in the presence of 100 μ M CaCl₂ or 2 mM EGTA or a mix containing 100 μ M CaCl₂ plus 50 μ M TG. 100% refers to the phosphorylation level in the presence of 100 μ M CaCl₂. Errors bars represent the standard error of 4 independent experiments. **B** – Reaction was performed at different free calcium concentrations obtained using an EGTA-CaCl₂ mix as determined with the CHELATOR program [50]. 100% refers to the phosphorylation level in the presence of 100 μ M CaCl₂. Errors bars represent the standard error of 3 independent experiments. Data were fitted By SigmaPlot using a Hill equation. Fitting parameters for SERCA1a: Hill number (h) = 1.29 +/- 0.17, r² = 0.9953; for SMA1: h = 1.34 +/- 0.25, r² = 0.9909. **C** - Phosphorylation assays were performed in the presence of 100 μ M CaCl₂ plus various concentrations of TG as indicated. 100% refers to the phosphorylation level in the presence of 100 μ M CaCl₂. Errors bars represent the standard error of 3 independent experiments. Data were fitted using a single ligand binding model for SERCA1a and a Hill equation for SMA1. Fitting parameters for SERCA1a: h = -1, r² = 0.9963; for SMA1: h = -1, r² = 0.9644. **D** – Phosphorylation assays were performed in the presence of 100 μ M CaCl₂ plus various concentrations of CPA as indicated. 100% refers to the phosphorylation intensity obtained by subtracting the phosphorylation intensity measured in the presence of 100 μ M CaCl₂ to that measured in the presence of 100 μ M CaCl₂ plus 50 μ M TG. Errors bars represent the standard error of 4 independent measurements for SERCA1a and 5 for SMA1. Data were fitted using a Hill equation. Fitting parameters for SERCA1a: h = -1, r² = 0.9908; for SMA1: h = -0.52 +/- 0.03, r² = 0.9964

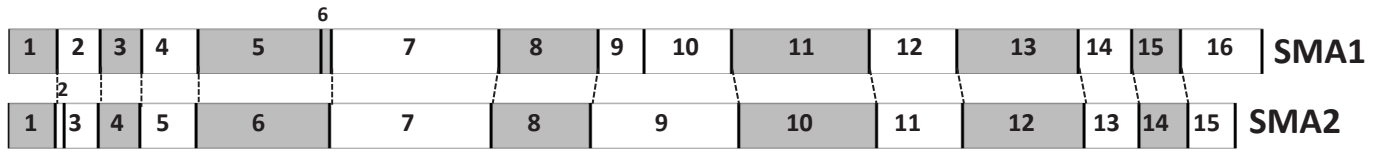
Supporting Information

S1 Table. List of the Ca²⁺-ATPases used in the phylogenetic analysis. Sequences are given with their accession number, their size in amino acids (aa), their originating organism, and the sequence of their N- and C-terminal ends.

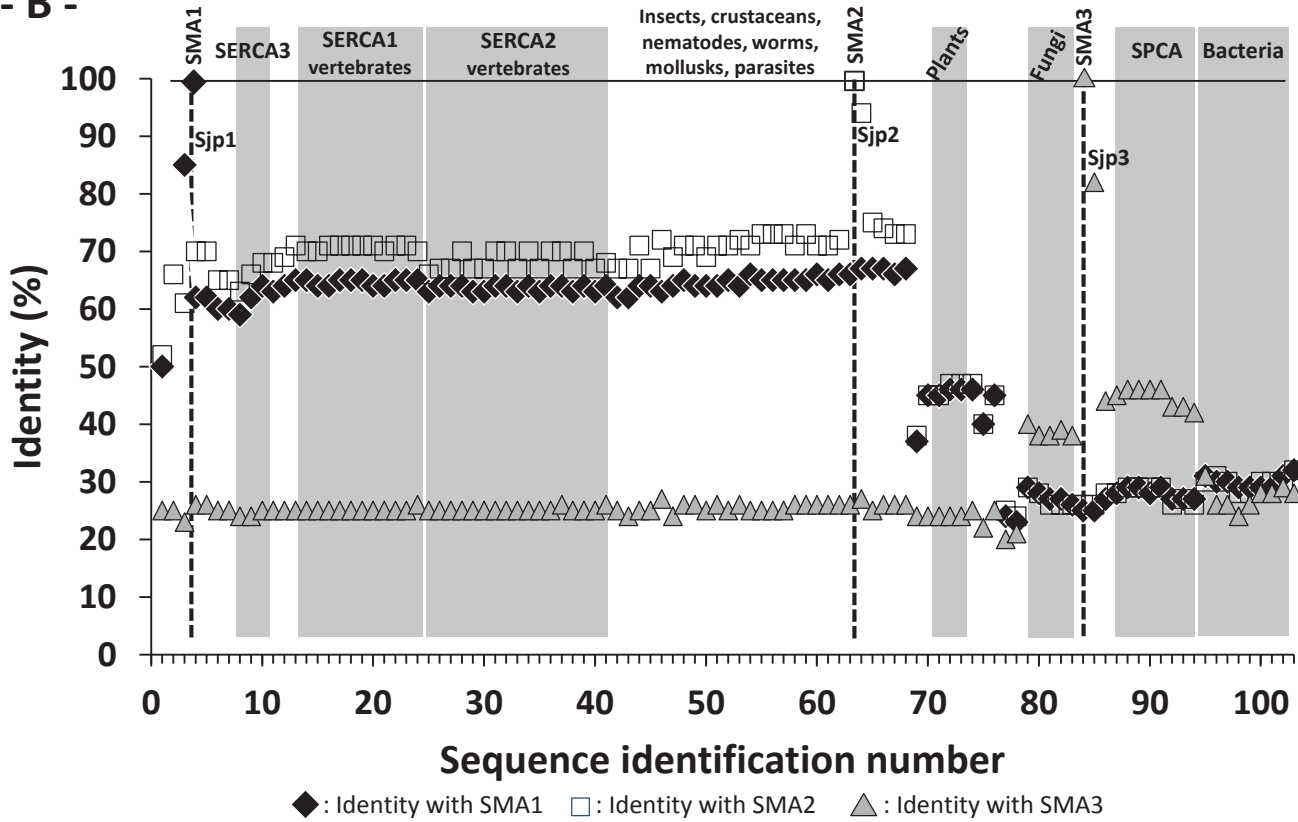
S2 Tables. TG and CPA binding sites in SERCA1a, PfATP6, SMA1 and SMA2.

S1 Fig. Relative expression levels of genes coding for SMA1 and SMA2. Normalized relative reads from RNA-seq data were taken from GeneDB. C: Cercariae; 3H: 3h-schistosomula; 24H: 24h-schistosomula; A: adult worm.

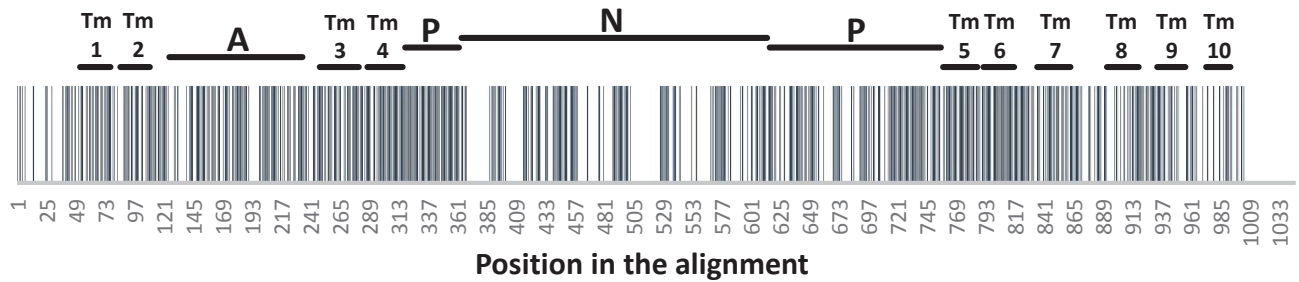
- A -



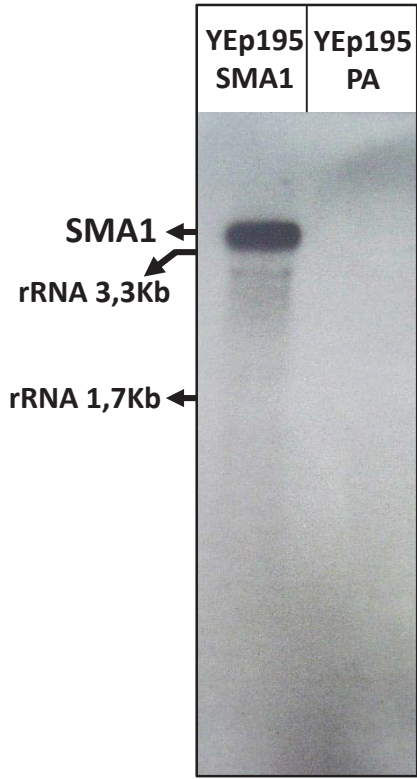
- B -



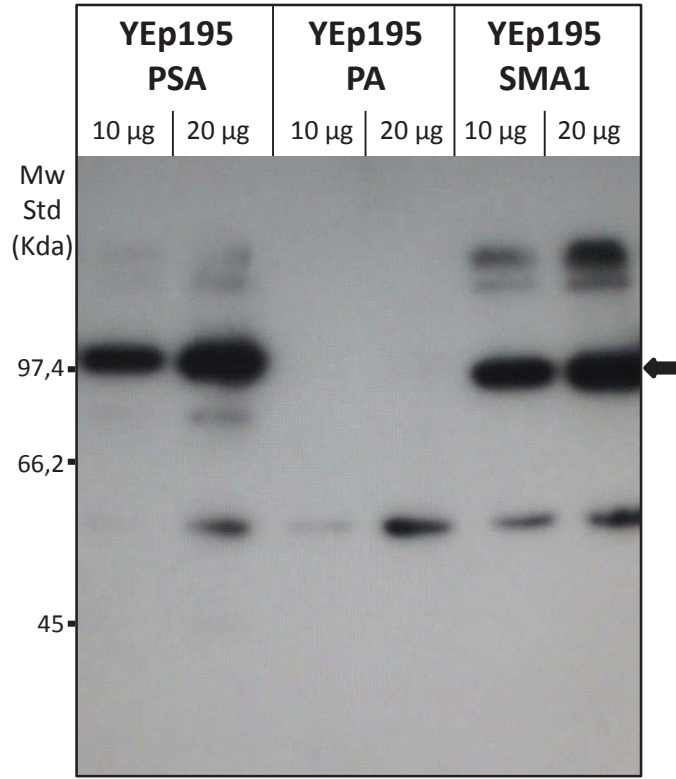
- C -



- A -



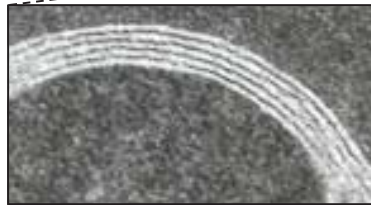
- B -



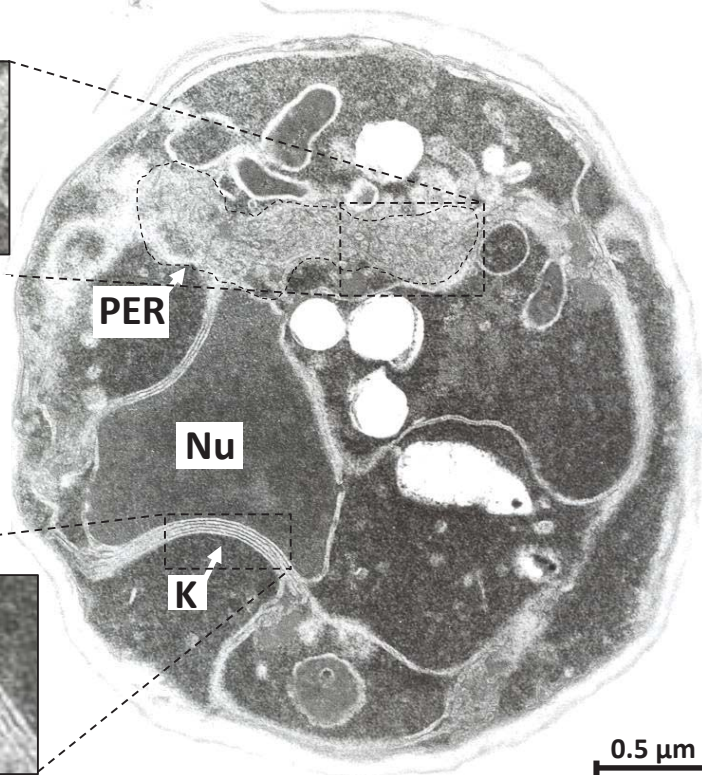
A



Proliferating Endoplasmic Reticulum



Karmellae



PER

Nu

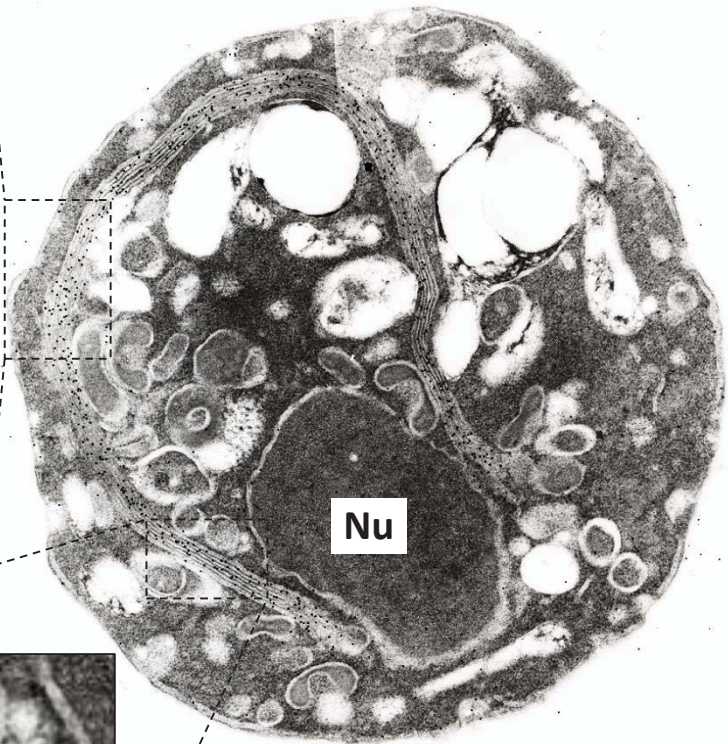
K

0.5 μm

B

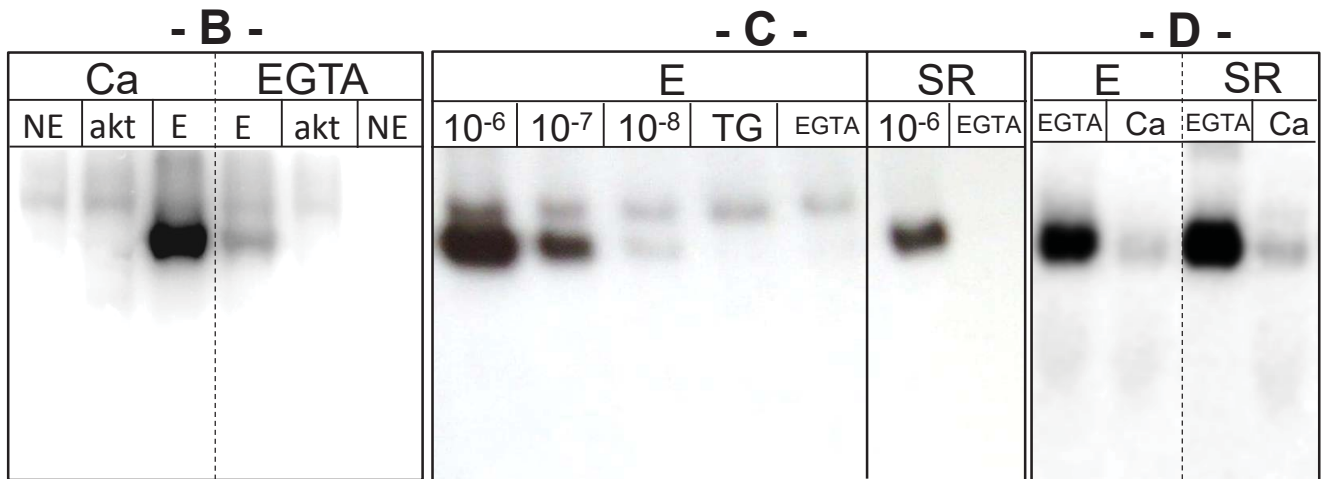
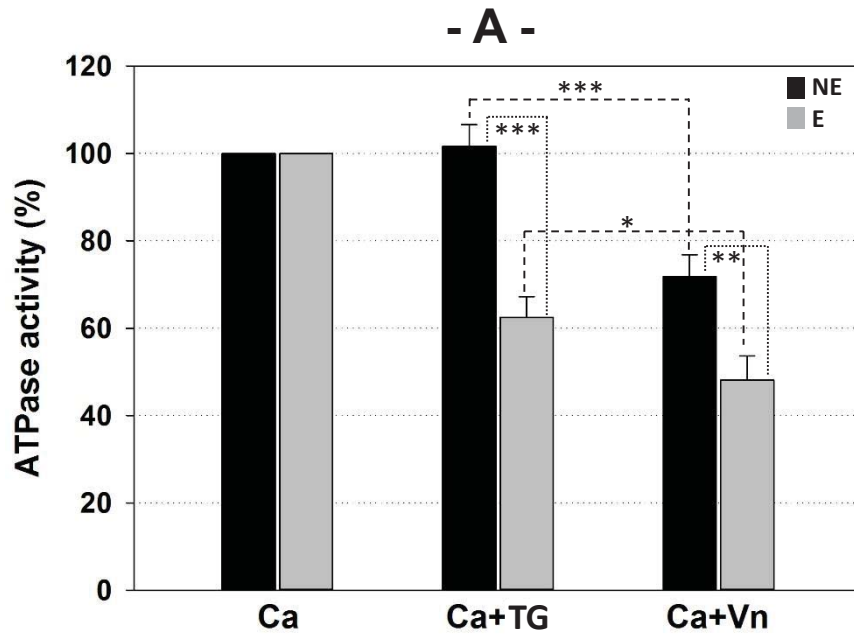


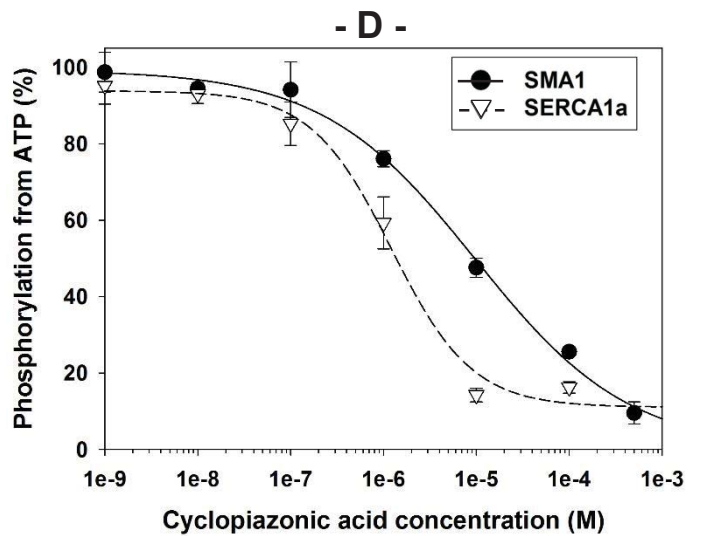
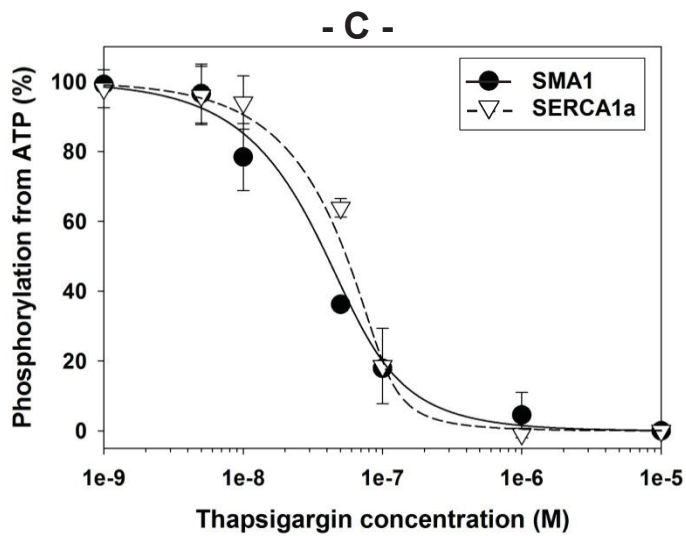
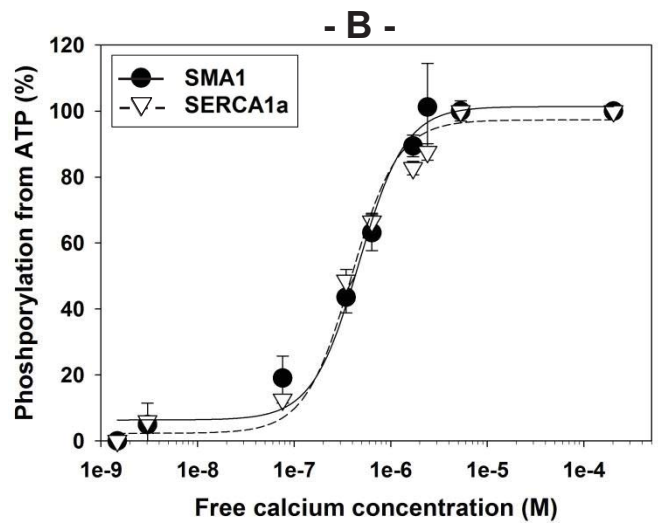
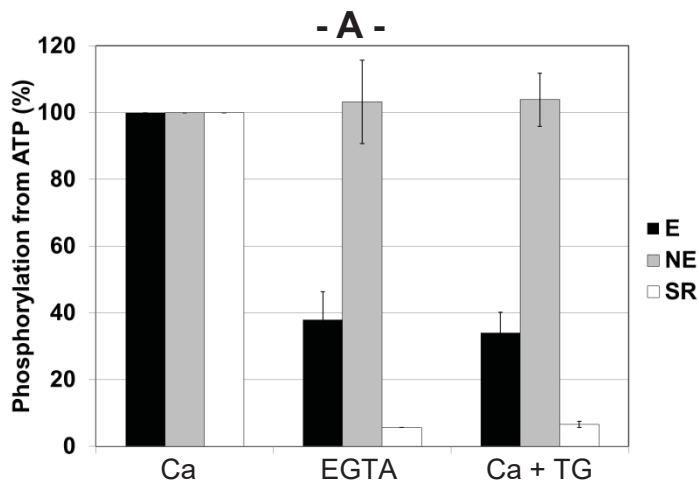
Immunolabelled Karmellae



Nu

0.5 μm





S1 Table. List of the Ca²⁺-ATPases used in the phylogenetic analysis

Seq	Accession	aa	Organism	N-terminus	C-terminus
1	NP_563860	998	Arabidopsis thaliana	MEDYA	DRRDK
4	XP_002127180	1000	Ciona intestinalis	MEDAY	LKKTQ
5	BAD18074	1000	Ciona savignyi	MENAY	TKKSQ
6	NP_777615	1043	Homo sapiens	MEAAH	VCTSD
7	NP_058025	1038	Mus musculus	MEEAH	VWPSD
8	P18596	1061	Rattus norvegicus	MEEAH	VSAAS
9	NP_990222	1042	Gallus gallus	MEAAH	TCNSD
10	NP_001088563	1033	Xenopus laevis	MDSAH	NNISK
11	NP_001072333	1033	Xenopus (Silurana) tropicalis	MDSAH	NNISK
12	P70083	996	Makaira nigricans	MENAH	GKEVK
13	XP_005156129	991	Danio rerio	MEDAH	NYVDV
14	Q92105	994	Pelophylax esculentus	MEQAH	NYLEG
15	CAC20853	994	Rana clamitans	MENAH	NYLDG
16	NP_990850	994	Gallus gallus	MENAH	NYLEA
17	XP_001502312	993	Equus caballus	MEAAH	NYLEG
18	NP_001069235	993	Bos taurus	MEAAH	NYLEG
19	XP_860120	993	Canis lupus familiaris	MEAAH	NYLEG
20	NP_001082787	1001	Oryctolagus cuniculus	MEAAH	DERRK
21	NP_775293	1001	Homo sapiens	MEAAH	DERRK
22	NP_031530	994	Mus musculus	MEAAH	NYLEG
23	NP_478120	994	Rattus norvegicus	MEAAH	NYLEG
24	XP_005166857	996	Danio rerio	MENAH	PAPED
25	NP_001086443	1042	Xenopus laevis	MENAH	EMFWS
26	NP_001258903	1042	Gallus gallus	MENAH	DMFWS
27	XP_002192568	1043	Taeniopygia guttata	MENAH	DMFWS
28	XP_007489917	997	Monodelphis domestica	MENAH	PAVLE
29	P20647	1042	Oryctolagus cuniculus	MENAH	DLLWS
30	NP_733765	1042	Homo sapiens	MENAH	DMFWS
31	XP_001141455	997	Pan troglodytes	MENAH	PAILE
32	XP_005217964	997	Bos taurus	MENAH	PAILE
33	NP_001075234	1042	Equus caballus	MENAH	DMFWS
34	CAA33169	997	Sus scrofa	MENAH	PAILE
35	NP_999030	1042	Sus scrofa	MENAH	DMFWS
36	NP_001003214	997	Canis lupus familiaris	MENAH	PAILE
37	NP_001009216	997	Felis catus	MENAH	PAILE
38	NP_001104293	1043	Rattus norvegicus	MENAH	DMFWS
39	NP_033852	998	Mus musculus	MENAH	PAILE
40	BAD90532	1044	Mus musculus	MENAH	DMFWS
41	XP_001639528	1005	Nematostella vectensis	MDLAH	KHKVD
42	XP_001896249	1065	Brugia malayi	MENAH	SHDLL
43	XP_002642312	1060	Caenorhabditis briggsae	MEDAH	LHNEL
44	NP_499385	1004	Caenorhabditis elegans	MEDAH	KDKRD
45	NP_001032719	1022	Strongylocentrotus purpuratus	MDLAH	IYYI
46	P35316	1003	Artemia franciscana	MEDAH	FSFIK
47	XP_002401874	977	Ixodes scapularis	KPLWQ	LCSPF
48	AAN77377	1002	Porcellio scaber	MENSH	IHKQW
49	AAB82291	1002	Procambarus clarkii	MDDAH	IKQQW
50	AAW22143	1020	Panulirus argus	MEDAH	KIYFF
51	XP_001868188	995	Culex quinquefasciatus	MEDGH	IKKWE
52	XP_316251	1018	Anopheles gambiae str. PEST	MEDGH	IWGP
53	XP_001652085	999	Aedes aegypti	MEDGH	IKKWD

54	XP_008185968	1023	<i>Acyrtosiphon pisum</i>	MEDAH	IYGPL
55	XP_002092715	1002	<i>Drosophila yakuba</i>	MEDGH	VVDRM
56	NP_476832	1002	<i>Drosophila melanogaster</i>	MEDGH	VVDRM
57	XP_002040177	1002	<i>Drosophila sechellia</i>	MEDGH	VVDRM
58	NP_001157948	1025	<i>Bombyx mori</i>	MEDAH	IYGPL
59	AAD09820	1000	<i>Heliothis virescens</i>	MEDAH	PTWKL
60	XP_966783	1019	<i>Tribolium castaneum</i>	MEDGH	CVSPI
61	XP_006565281	1020	<i>Apis mellifera</i>	MEDGH	IYPI
62	XP_008209464	1002	<i>Nasonia vitripennis</i>	MEDAH	VKPVH
65	ACX35338	1004	<i>Lumbricus rubellus</i>	MEEAH	MSEKN
66	ABS19815	1007	<i>Pinctada fucata</i>	MENAH	ATKMD
67	AAC63909	994	<i>Placopecten magellanicus</i>	MEYAH	KFTDA
68	BAA37143	993	<i>Mizuhopecten yessoensis</i>	MEYAH	KFTDA
69	AAB17958	981	<i>Trichomonas vaginalis</i>	MVYPA	HIVRE
70	NP_172259	1061	<i>Arabidopsis thaliana</i>	MGKGS	KQKEE
71	NP_172246	1061	<i>Arabidopsis thaliana</i>	MGKGG	KQKEE
72	NP_191999	1054	<i>Arabidopsis thaliana</i>	MEEK	KIKTM
73	NP_001234073	1048	<i>Solanum lycopersicum</i>	MEEKP	KLKAA
74	P54209	1037	<i>Dunaliella bioculata</i>	MVSHA	ALKLK
75	AAC47505	1031	<i>Leishmania amazonensis</i>	MSKLQ	SRIWN
76	P35315	1011	<i>Trypanosoma brucei brucei</i>	MLPEN	EKKKD
77	WP_009885927	874	<i>Mycoplasma genitalium</i>	MNSWT	GYGNI
78	WP_010874566	872	<i>Mycoplasma pneumoniae</i>	MNKWT	SYGSV
79	NP_595098	899	<i>Schizosaccharomyces pombe</i> 972h-	MSVQY	LLRNV
80	XP_503736	928	<i>Yarrowia lipolytica</i> CLIB122	MDSHT	TNSVV
81	AAC68831	918	<i>Ogataea angusta</i>	MASDN	YSTSV
82	NP_011348	950	<i>Saccharomyces cerevisiae</i> S288c	MSDNP	YFSNV
83	CAA04476	936	<i>Kluyveromyces lactis</i>	MSDNP	SSSIV
86	NP_001021862	978	<i>Caenorhabditis elegans</i>	MIETL	SVSGI
87	NP_786979	953	<i>Bos taurus</i>	MDNLL	SFLEV
88	NP_055197	919	Human	MKVAR	SFLEV
89	Q5R5K5	918	<i>Pongo abelii</i>	MKVAR	SFLEV
90	NP_778190	918	<i>Mus musculus</i>	MKVAR	SFLEV
91	Q64566	919	<i>Rattus norvegicus</i>	MKVAR	SFLEV
92	O75185	946	Human	MVEGR	HPEDV
93	NP_081198	944	<i>Mus musculus</i>	MGRRL	LPEAV
94	NP_604457	944	<i>Rattus norvegicus</i>	MGRRF	LPEAV
95	WP_010876632	844	<i>Methanothermobacter thermautotrophicus</i>	MFKMK	ERANP
96	WP_010905909	878	<i>Lactococcus lactis</i>	MQPYN	VFEKH
97	WP_003721406	880	<i>Listeria monocytogenes</i>	MEIYR	NKFFK
98	WP_010872526	905	<i>Synechocystis</i> sp. PCC 6803	MDFPT	NRLDP
99	WP_003410027	905	<i>Mycobacterium tuberculosis</i>	MVTRA	RAQPP
100	WP_010873968	945	<i>Synechocystis</i> sp. PCC 6803	MKACC	YSSFK
101	P37278	926	<i>Synechococcus elongatus</i> PCC 7942	MKGAI	RQRRY
102	WP_003232087	890	<i>Bacillus subtilis</i>	MKFHE	LTRKK
103	WP_000073702	888	<i>Bacillus cereus</i>	MSNWY	LAKKN

Tables S2

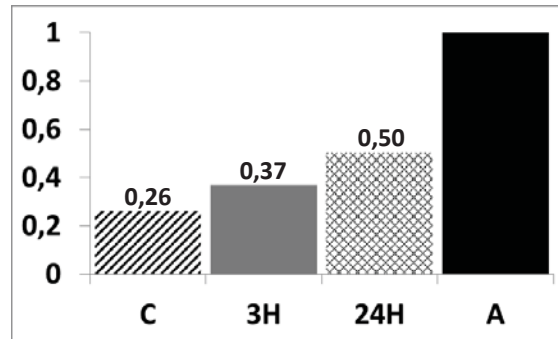
TG binding site. Information about SERCA1a and PfATP6 comes from [51].

SERCA1a	PfATP6	SMA1	SMA2
L ²⁵³	I ²⁶¹	I ²⁵⁴	L ²⁵³
E ²⁵⁵	L ²⁶³	E ²⁵⁶	E ²⁵⁵
F ²⁵⁶	F ²⁶⁴	F ²⁵⁷	F ²⁵⁶
Q ²⁵⁹	Q ²⁶⁷	Q ²⁶⁰	Q ²⁵⁹
L ²⁶⁰	L ²⁶⁸	L ²⁶¹	L ²⁶⁰
V ²⁶³	I ²⁷¹	V ²⁶⁴	V ²⁶³
I ²⁶⁷	I ²⁷⁵	I ²⁶⁸	I ²⁶⁷
A ³⁰⁶	A ³¹³	A ³⁰⁷	A ³⁰⁶
I ⁷⁶⁵	I ⁹⁷⁶	I ⁷⁶⁷	I ⁷⁷⁴
N ⁷⁶⁸	N ⁹⁷⁹	N ⁷⁷⁰	N ⁷⁷⁷
V ⁷⁶⁹	I ⁹⁸⁰	I ⁷⁷¹	I ⁷⁷⁸
V ⁷⁷²	V ⁹⁸³	V ⁷⁷⁴	V ⁷⁸¹
F ⁷⁷⁶	F ⁹⁸⁸	F ⁷⁷⁸	F ⁷⁸⁵
L ⁸²⁸	L ¹⁰³⁹	L ⁸³⁰	L ⁸³⁷
I ⁸²⁹	I ¹⁰⁴⁰	I ⁸³¹	I ⁸³⁸
F ⁸³⁴	L ¹⁰⁴⁵	F ⁸³⁶	F ⁸⁴³
Y ⁸³⁷	Y ¹⁰⁴⁸	Y ⁸³⁹	Y ⁸⁴⁶
M ⁸³⁸	I ¹⁰⁴⁹	M ⁸⁴⁰	V ⁸⁴⁷

CPA binding site. Information about SERCA1a and PfATP6 comes from [51].

SERCA1a	PfATP6	SMA1	SMA2
Q ⁵⁶	Q ⁶⁰	Q ⁵⁷	Q ⁵⁶
D ⁵⁹	D ⁶³	D ⁶⁰	D ⁵⁹
L ⁶¹	L ⁶⁵	L ⁶²	L ⁶¹
V ⁶²	V ⁶⁶	V ⁶³	V ⁶²
L ⁶⁵	L ⁶⁹	L ⁶⁶	L ⁶⁵
L ⁹⁸	L ¹⁰⁴	L ⁹⁹	L ⁹⁸
N ¹⁰¹	N ¹⁰⁷	N ¹⁰²	N ¹⁰¹
A ¹⁰²	A ¹⁰⁸	A ¹⁰³	A ¹⁰²
L ²⁵³	I ²⁶¹	I ²⁵⁴	L ²⁵³
I ³⁰⁷	I ³¹⁴	I ³⁰⁸	I ³⁰⁷
E ³⁰⁹	E ³¹⁶	E ³¹⁰	E ³⁰⁹
p ³¹²	p ³¹⁹	p ³¹³	p ³¹²

Smp 007260.1 (SMA1)



Smp 136710 (SMA2)

